

Size-dependent strain relaxation in InN islands grown on GaN by metalorganic chemical vapor deposition

Wen-Che Tsai, Feng-Yi Lin, Wen-Cheng Ke, Shu-Kai Lu, Shun-Jen Cheng, Wu-Ching Chou, Wei-Kuo Chen, Ming-Chih Lee, and Wen-Hao Chang

Citation: *Applied Physics Letters* **94**, 063102 (2009); doi: 10.1063/1.3064166

View online: <http://dx.doi.org/10.1063/1.3064166>

View Table of Contents: <http://scitation.aip.org/content/aip/journal/apl/94/6?ver=pdfcov>

Published by the [AIP Publishing](#)

Articles you may be interested in

[Effects of grain size on the mosaic tilt and twist in InN films grown on GaN by metal-organic chemical vapor deposition](#)

Appl. Phys. Lett. **89**, 092114 (2006); 10.1063/1.2345224

[In-rich InGaN GaN quantum wells grown by metal-organic chemical vapor deposition](#)

J. Appl. Phys. **99**, 044906 (2006); 10.1063/1.2173043

[In situ observation of coalescence-related tensile stresses during metalorganic chemical vapor deposition of GaN on sapphire](#)

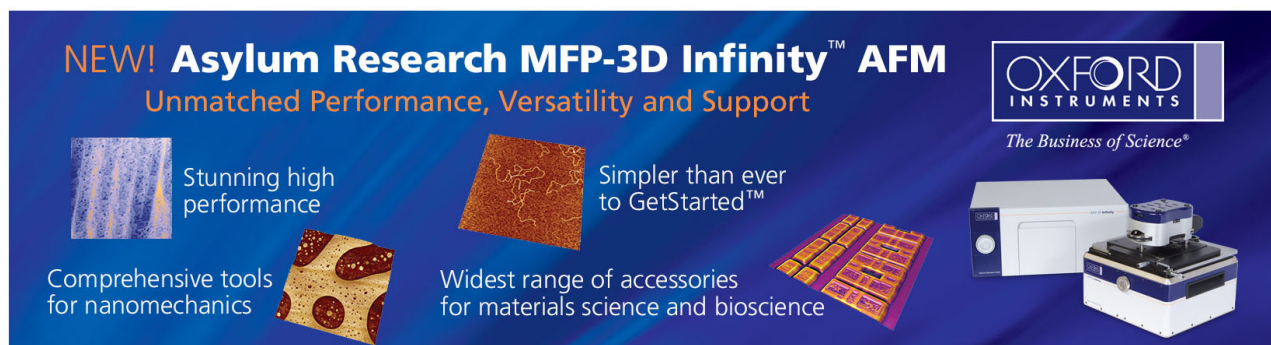
Appl. Phys. Lett. **86**, 261907 (2005); 10.1063/1.1968436

[Effects of growth interruption on the optical and the structural properties of InGaN/GaN quantum wells grown by metalorganic chemical vapor deposition](#)

J. Appl. Phys. **90**, 5642 (2001); 10.1063/1.1410320

[Strain relief and its effect on the properties of GaN using isoelectronic In doping grown by metalorganic vapor phase epitaxy](#)

Appl. Phys. Lett. **75**, 4106 (1999); 10.1063/1.125551

The advertisement features a dark blue background with white and orange text. At the top left, it reads 'NEW! Asylum Research MFP-3D Infinity™ AFM' in large white letters, followed by 'Unmatched Performance, Versatility and Support' in orange. To the right is the Oxford Instruments logo, which includes the text 'OXFORD INSTRUMENTS' and 'The Business of Science®'. Below the text are several images: a 3D surface plot, a textured surface, a grid of small images, and the physical AFM instrument. Text boxes describe the instrument's capabilities: 'Stunning high performance', 'Simpler than ever to GetStarted™', 'Comprehensive tools for nanomechanics', and 'Widest range of accessories for materials science and bioscience'.

Size-dependent strain relaxation in InN islands grown on GaN by metalorganic chemical vapor deposition

Wen-Che Tsai, Feng-Yi Lin, Wen-Cheng Ke, Shu-Kai Lu, Shun-Jen Cheng, Wu-Ching Chou, Wei-Kuo Chen, Ming-Chih Lee, and Wen-Hao Chang^{a)}
Department of Electrophysics, National Chiao Tung University, Hsinchu 300, Taiwan

(Received 6 November 2008; accepted 12 December 2008; published online 9 February 2009)

We report Raman measurements on InN islands grown on GaN by metalorganic chemical vapor deposition. The Raman frequency of the InN E_2 mode is found to decrease exponentially with the island's aspect ratio, indicating a size dependent strain relaxation during the island formation. Our results suggest that most of the strain at the InN–GaN interface have been released plastically during the initial stage of island formations. After that, the residual strain of only -3.5×10^{-3} is further relaxed elastically via surface islanding. The experimental data are in agreement with the strain relaxation predicted from a simplified model analysis as well as three-dimensional finite-element simulations. © 2009 American Institute of Physics. [DOI: 10.1063/1.3064166]

Recently, the band gap energy of InN was found to be near 0.7 eV (Refs. 1–3) rather than the previously accepted value of about 1.9 eV. This finding makes the indium containing nitrides very appealing due to their potential applications in the near infrared range. Beside the InN thin film growth, the fabrication of InN nanostructures also progress rapidly^{4–11} since the combination with GaN or AlN is expected to form low-dimensional systems with large quantum confinement. However, the large lattice misfit ($\sim 10\%$ – 13%) between InN and GaN or AlN further complicated the epitaxial growth of InN heterostructures. Many experimental evidences indicated that the strain of uncapped InN/GaN islands is almost fully relaxed by the formation of misfit dislocation (MD) networks at the InN–GaN interface.^{12,13} However, it is less clear whether and how the residual strain further releases via surface islanding. In our previous works, we have demonstrated that InN islands with controlled size and density can be formed on GaN by using different precursor injection schemes in metalorganic chemical vapor deposition (MOCVD).^{7,8} Good optical quality has been achieved by growth optimizations.¹¹ A further understanding and subsequent control of strain relaxation in InN/GaN islands and the relationship with their size and shape become important subjects for the development of prospective InN-based photonic devices.

In this letter, we report Raman measurements on InN/GaN islands of various sizes and shapes grown by MOCVD using different growth conditions. The Raman frequency is found to shift with the island size, indicating a size-dependent strain relaxation during the island formation. We show that the residual strain after plastic relaxation at the InN–GaN interface is further relieved elastically via surface islanding.

Samples were grown on (0001) sapphire by MOCVD using trimethylgallium, trimethylindium (TMIn), and ammonia (NH₃) as precursors. After the growth of a 2 μm GaN buffer layer at 1120 °C, the temperature was lowered to 625–700 °C for growing InN islands. Different gas-flow sequences and growth temperatures were used to control the

InN island size. Two series of samples were prepared. The first series was grown by the so-called flow-rate modulation epitaxy (FME) using alternately injected TMIn [0.15 slm (slm denotes standard liters per minute)] and NH₃ (18 slm) gas flows. A small NH₃ background flow (0.5 slm) was supplied during the TMIn periods.⁸ Three FME samples were grown at 625, 650, and 700 °C. Another series were grown by the same gas-flow sequence except that a high NH₃ background flow (10 slm) was used. Such a growth method is similar to the so-called pulsed mode (PM), where the NH₃ flow rate was kept high, but the TMIn was pulsed injected. Three PM samples have been grown at 700 °C using different TMIn injection times $t_{\text{in}} = 10, 15, \text{ and } 20$ s to control the island size. The details of the gas flow sequence can be found in Refs. 7 and 8. Surface morphology was investigated by atomic force microscopy (AFM). Raman measurements were carried out at room temperature in backscattering geometry (*c*-axis) using the 488 nm line of an Ar⁺ laser focused through a microscope objective into a spot of ~ 2 μm . The scattering light was analyzed by a 1 m double monochromator with a spectral resolution of 0.9 cm^{-1} and a peak uncertainty of about ± 0.2 cm^{-1} .

Figures 1(a) and 1(b) show the typical surface morphology of InN islands grown at 700 °C by using the PM and the

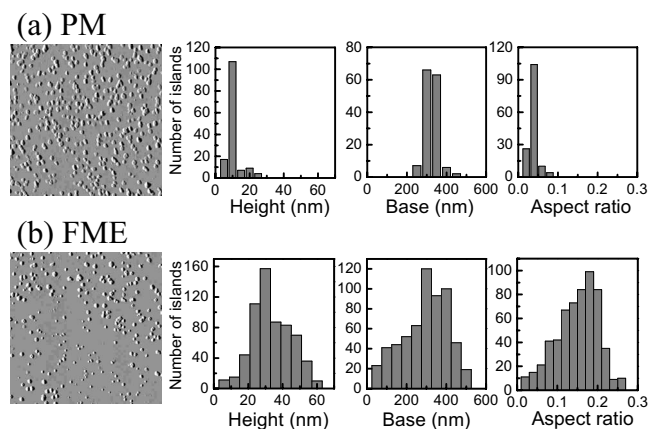


FIG. 1. AFM images (10×10 μm^2) and dots size distribution of InN islands grown by (a) the PM and (b) the FME at 700 °C.

^{a)} Author to whom correspondence should be addressed. Electronic mail: whchang@mail.nctu.edu.tw.

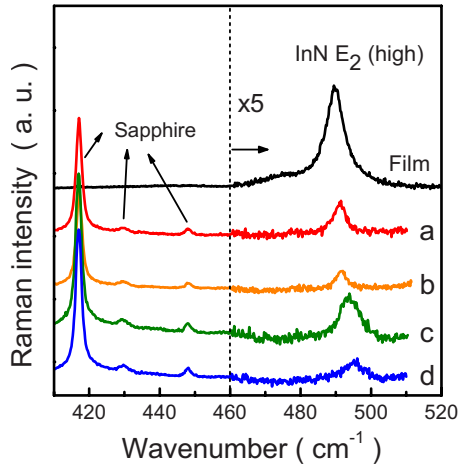


FIG. 2. (Color online) Four representative Raman spectra for InN islands of different sizes grown by the FME [(a) and (b)] and the PM [(c) and (d)] methods. The average island height (base diameter) for (a), (b), (c), and (d) are 47 (202), 38 (180), 22 (310), and 11 (320) nm, respectively. A spectrum taken from a 300 nm InN film is also included.

FME methods, respectively. The island's shape is hexagonal with a truncated flat top and steep faceted sidewalls. As shown in Fig. 1(a), the PM-grown islands have rather good size uniformity with flat shape and a typical aspect ratio (height/base) less than 0.05, depending on the depositing time. However, for the FME-grown islands, the size distribution is widespread. For the sample shown in Fig. 1(b), the island height (diameter) is from 6 to 60 nm (50 to 500 nm), with an aspect ratio ranging from 0.02 to 0.26. Such a widespread size distribution allowed us to study InN islands of different sizes and shapes on the same wafer, so that the influence of growth conditions, particularly the growth temperature, on the strain state can be examined. In our Raman measurements, the laser illuminating spot covers a total of ~ 10 – 20 individual islands. In order to know the size distribution within the laser spot, we have fabricated an array of markers on the sample surface. This helped us to precisely control the position of laser spot with an accuracy better than $0.5 \mu\text{m}$, so that the information about the island size can be obtained from AFM analysis. By inspecting different areas on the wafer, it is possible to locate some particular region where the island sizes are similar. Accordingly, Raman spectra for InN islands of different sizes were obtained.

In Fig. 2, four representative Raman spectra for different island sizes grown either by the PM or the FME are displayed, together with a spectrum obtained from a 300 nm InN thin film. Beside the sapphire peaks, the InN E_2 -high mode near 490 cm^{-1} can be observed. The Raman frequencies of InN islands are higher than that of the InN film, indicating that islands are more compressively strained than the thin film. In particular, we found that the Raman frequency of the InN islands redshifts with the increasing island size, indicating a size-dependent strain relaxation in the InN islands.

Figure 3(a) shows the measured E_2 -high-mode frequency of InN islands as a function of their aspect ratio (γ). A redshift in the Raman frequency with the increasing γ can be seen, regardless of how the InN islands were grown. In fact, we have also analyzed the Raman frequency as a function of island's height or diameter,¹⁴ but the data are more scattered. This leads us to infer that the decreasing

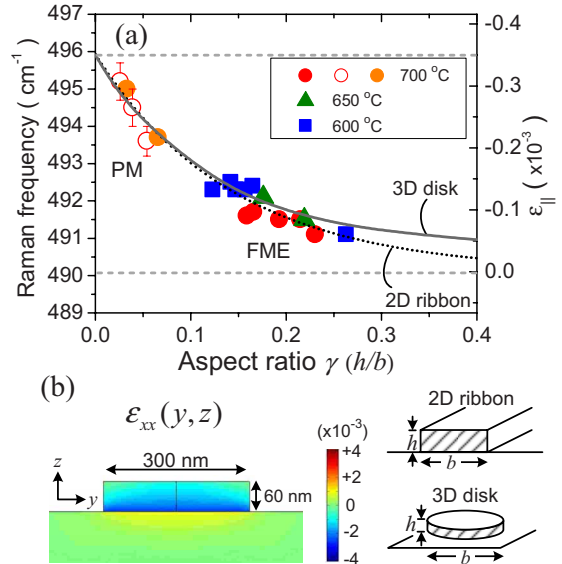


FIG. 3. (Color online) (a) The measured Raman frequency as a function of aspect ratio. The solid (hollow and half-filled) symbols are data obtained from FME (PM) samples grown at different temperatures. The hollow circles with error bars are from PM grown islands with $t_{\text{In}}=10, 15,$ and 20 s . The two half-filled circles are from different regions of the sample with $t_{\text{In}}=10 \text{ s}$. The dotted line is the exponential fitting curve. The solid line is the average in-plane strain in disk-shaped islands calculated from 3D finite-element simulations. (b) Simulated distribution of ϵ_{xx} in the y - z plane of an uncapped disk-shape island.

E_2 -high-mode frequency with the island aspect ratio appears to be a general trend.

The measured Raman shifts can be used to determine the in-plane strain ϵ_{\parallel} in the InN islands of different sizes. Here we adopt the values reported in Ref. 15, where the strain-free Raman frequency and the slope coefficient $\Delta\omega/\Delta\epsilon_{\parallel}$ of the InN E_2 -high mode was determined to be 490.1 cm^{-1} and $-1660 \pm 140 \text{ cm}^{-1}$, respectively. As shown by the right scale of Fig. 3(a), the in-plane strain ϵ_{\parallel} of these InN islands is compressive (negative), decreasing from -3.1×10^{-3} to -0.6×10^{-3} with the increasing γ from 0.026 to 0.26. It can be inferred that the in-plane strain would approach zero for $\gamma \gg 1$, i.e., the limiting case of a columnlike structure. On the other hand, as $\gamma \sim 0$ (i.e., an infinite platelet structure), the measured in-plane strain would represent the initial strain ϵ_{\parallel}^0 at the InN–GaN interface. If we use the exponential function $\epsilon_{\parallel}(\gamma) = \epsilon_{\parallel}^0 \exp(-\lambda\gamma)$ with λ as a fitting parameter to approximate the decreasing in-plane strain, the initial strain can be determined to be $\epsilon_{\parallel}^0 = -3.5 \times 10^{-3}$, with the parameter $\lambda = 6.9$. Since the theoretical lattice misfit for this heterosystem is $f = (a_{\text{GaN}} - a_{\text{InN}})/a_{\text{InN}} = -0.0971$,¹³ the deduced ϵ_{\parallel}^0 indicated that at least 96% of the interface strain has been released at the initial stage of island formations. This result is in good agreement with that deduced from the analysis of moiré fringes in high-resolution transmission electron microscopy images by Lozano *et al.*,^{12,13} where the degree of plastic relaxation was estimated to be 98% due to the formation of MD networks at the InN–GaN interface.

The decreasing in-plane strain with the island's aspect ratio indicates that the residual strain (after the initial plastic relaxation) was further released elastically via surface islanding. In order to know how the residual strain was released via the island's free borders, we consider the ribbon model proposed by Kern and Muller.¹⁶ Although this two-dimensional

(2D) model is limited to elongated ribbons, it simplifies the problem considerably due to the availability of analytical expression, so that a good approximation for the relaxation of the topmost layers of the InN islands can be obtained.¹⁷ In the model, the in-plane strain in an infinitely long ribbon of height h and base b is given by

$$\varepsilon_{\parallel}(\gamma, N) = \varepsilon_{\parallel}^0 \langle M_1 \rangle^{N-1}, \quad (1)$$

$$\langle M_1 \rangle = 1 - \frac{2\pi\gamma}{N} + \left(1 + \sqrt{\frac{2\pi\gamma}{N}}\right)^2 \exp\left(-\sqrt{\frac{2N}{\gamma\pi}}\right), \quad (2)$$

where N is the number of monolayers and $\gamma = h/b$ is the aspect ratio. The equations illustrate that the relaxation depends on both γ and N , while our data [Fig. 3(a)] are a function of γ only. This means that the equations should be further simplified. For the islands sizes investigated here, i.e., $0.02 < \gamma < 0.3$ and $N \geq 28$ ($h \geq 8$ nm), the exponential term in $\langle M_1 \rangle$ is negligible, so that Eq. (1) can be reduced to $\varepsilon_{\parallel}(\gamma, N) = \varepsilon_{\parallel}^0 (1 - 2\pi\gamma/N)^{N-1}$. Numerically, as $N > 10$, the expression can be approximated by an exponential function,

$$\varepsilon_{\parallel}(\gamma) = \varepsilon_{\parallel}^0 \exp(-2\pi\gamma), \quad (3)$$

which is a function of γ only and independent of N . This explains why the observed in-plane strain decreases exponentially with the aspect ratio. The fitted λ value is also close to 2π , consistent with this simplified model analysis.

The three-dimensional (3D) strain distribution in an uncapped island has also been calculated based on the finite-element method.¹⁸ For simplicity, we consider a disk-shaped InN island formed on the GaN surface, with a residual strain of $\varepsilon_{\parallel}^0 = -3.5 \times 10^{-3}$ at the InN–GaN interface. The simulated strain distribution of ε_{xx} in the y - z plane is shown in Fig. 3(b), where a nonuniform distribution can be seen. By taking the average of the in-plane strain over the entire disk, the calculated results can be compared with the measured Raman data. As shown in Fig. 3(a), the simulated result (solid line) agrees well with the experimental data, further confirming our assertion of size-dependent strain relaxations.

In summary, strain relaxation in uncapped InN/GaN islands of different sizes have been investigated by Raman measurements. A redshift in the Raman peak with the island's aspect ratio was observed, regardless of how the InN islands were grown. Most of the strain at the InN–GaN interface was released plastically, with a relaxation degree up to $>96\%$, during the initial stage of island formations. After

that, the residual strain of only -3.5×10^{-3} was further relaxed elastically via the surface islanding. Based on a simplified 2D model analysis and full 3D simulations, we established the relationship of the strain relaxation in InN/GaN islands with their size and shape.

This work was supported in part by the project of MOE-ATU and the National Science Council of Taiwan under Grant Nos. NSC 97-2112-M-009-015-MY2, NSC 97-2112-M-009-018, NSC 96-2112-M-009-026-MY3, and NSC 95-2112-M-009-044-MY3.

- ¹V. Yu. Davydov, A. A. Klochikhin, R. P. Seisyan, V. V. Emtsev, S. V. Ivanov, F. Bechstedt, J. Furthmüller, H. Harima, A. V. Mudryi, J. Aderhold, O. Semchinova, and J. Graul, *Phys. Status Solidi B* **229**, R1 (2002).
- ²J. Wu, W. Walukiewicz, K. M. Yu, J. W. Ager III, E. E. Haller, H. Lu, W. J. Schaff, Y. Saito, and Y. Nanishi, *Appl. Phys. Lett.* **80**, 3967 (2002).
- ³T. Matsuoka, H. Okamoto, M. Nakao, H. Harima, and E. Kurimoto, *Appl. Phys. Lett.* **81**, 1246 (2002).
- ⁴Y. F. Ng, Y. G. Cao, M. H. Xie, X. L. Wang, and S. Y. Tong, *Appl. Phys. Lett.* **81**, 3960 (2002).
- ⁵O. Briot, B. Maleyre, and S. Ruffenach, *Appl. Phys. Lett.* **83**, 2919 (2003).
- ⁶A. Yoshikawa, N. Hashimoto, N. Kikukawa, S. B. Che, and Y. Ishitani, *Appl. Phys. Lett.* **86**, 153115 (2005).
- ⁷W. C. Ke, C. P. Fu, C. Y. Chen, L. Lee, C. S. Ku, W. C. Chou, W.-H. Chang, M. C. Lee, W. K. Chen, W. J. Lin, and Y. C. Cheng, *Appl. Phys. Lett.* **88**, 191913 (2006).
- ⁸W. C. Ke, L. Lee, C. Y. Chen, W. C. Tsai, W.-H. Chang, W. C. Chou, M. C. Lee, W. K. Chen, W. J. Lin, and Y. C. Cheng, *Appl. Phys. Lett.* **89**, 263117 (2006).
- ⁹L. Zhou, T. Xu, J. Smith, and T. D. Moustakas, *Appl. Phys. Lett.* **88**, 231906 (2006).
- ¹⁰S. Ruffenach, O. Briot, M. Moret, and B. Gil, *Appl. Phys. Lett.* **90**, 153102 (2007).
- ¹¹W.-H. Chang, W. C. Ke, S. H. Yu, L. Lee, C. Y. Chen, W. C. Tsai, W. C. Chou, M. C. Lee, and W. K. Chen, *J. Appl. Phys.* **103**, 104306 (2008).
- ¹²J. G. Lozano, A. M. Sanchez, R. Garcia, D. Gonzalez, O. Briot, and S. Ruffenach, *Appl. Phys. Lett.* **88**, 151913 (2006).
- ¹³J. G. Lozano, A. M. Sánchez, R. García, D. González, M. Herrera, N. D. Browning, S. Ruffenach, and O. Briot, *Appl. Phys. Lett.* **91**, 071915 (2007).
- ¹⁴F. Demangeot, J. Frandon, C. Piquier, M. Caumont, O. Briot, B. Maleyre, S. Clur-Ruffenach, and B. Gil, *Phys. Rev. B* **68**, 245308 (2003).
- ¹⁵X. Wang, S. B. Che, Y. Ishitani, and A. Yoshikawa, *Appl. Phys. Lett.* **89**, 171907 (2006).
- ¹⁶R. Kern and P. Müller, *Surf. Sci.* **392**, 103 (1997).
- ¹⁷V. Lebedev, V. Cimalla, J. Pezoldt, M. Himmerlich, S. Krischok, J. A. Schaefer, O. Ambacher, F. M. Morales, J. G. Lozano, and D. Gonzalez, *J. Appl. Phys.* **100**, 094902 (2006).
- ¹⁸The 3D strain simulation is performed using the finite-element package COMSOL MULTIPHYSICS®.